J. Fluid Mech. (1964), *vol.* 20, *part* 3, *pp.* 383–399
Printed in Great Britain

The unsteady flow within a spinning cylinder

By E. H. WEDEMEYER

U.S.A. Ballistic Research Laboratories, Aberdeen Proving Ground,
Aberdeen, Md.

(Received 13 March 1964)

A theoretical analysis is given of the unsteady flow of a liquid within a cylinder of finite length started suddenly so as to spin about its axis. It is found that a secondary flow, caused by the end walls of the cylindrical container, has a strong effect on the generation of spin in the liquid. In the vicinity of the end walls the fluid motion is characterized by a boundary-layer flow, which can be either laminar or turbulent. The fluid within the boundary layers rotates faster than that at a large distance from the end walls, and therefore is thrown, by centrifugal forces, radially outwards. The radial outflow in the boundary layer creates a slow secondary motion within the spinning liquid. Due to the secondary flow, the transport of angular momentum from the walls to the interior is accomplished by convection rather than diffusion. A treatment is given for both laminar and turbulent end-wall boundary layers. The theoretical results are compared with experimental observations and good agreement is found.

1. Introduction

It is well known that spin-stabilized shells can become dynamically unstable if they are filled with a liquid. According to a theoretical analysis of Stewartson (1959), the stability of a shell containing a cylindrical liquid-filled cavity can be predicted if the liquid is in rigid-body rotation.

However, for a liquid of small viscosity, a relatively long time is required for the liquid to reach full spin, and, during the transition period, the shell might become dynamically unstable even though it might be stable at its final state if the liquid attained rigid-body rotation. In the course of experimental investigations (Karpov 1962), severe dynamic instabilities of liquid-filled spinning shells have been observed in cases where the shell should have been stable according to Stewartson's theory and the assumption of rigid rotation of the liquid filler. In order to extend the prediction of instabilities in such cases, it appeared desirable to analyse the problem of unsteady fluid motion within a cylinder, suddenly started spinning about its axis.

If the cylinder is infinitely long, a solution to the problem is obtained without difficulty, but the expectation that this solution might be approximately valid for slender but finite cylinders proves to be wrong. It is found that the effect of the cylinder ends on the fluid motion is not only not negligible, but dominating. The fluid motion is entirely changed by the presence of a secondary flow induced by the cylinder ends. The secondary flow convects spinning fluid from the walls into the interior of the cylinder and, as a consequence, the fluid attains rotational motion many times faster than without secondary flow. In the following, a theoretical analysis is given of the unsteady flow within a cylinder which is started spinning about its axis of rotation. The results are then compared with some experimental data obtained: (1) from spin decay data of liquid-filled shells; and (2) from direct observations of the secondary flow within a spinning transparent cylinder.

2. Theoretical analysis of the flow

2.1. *Structure of the secondary flow*

The diagram in figure 1 shows an axial section and a cross-section of the spinning cylinder. The height of the cylinder is h, the radius a. In the following analysis, we use a polar co-ordinate system θ, r, z with the origin in the centre as shown in

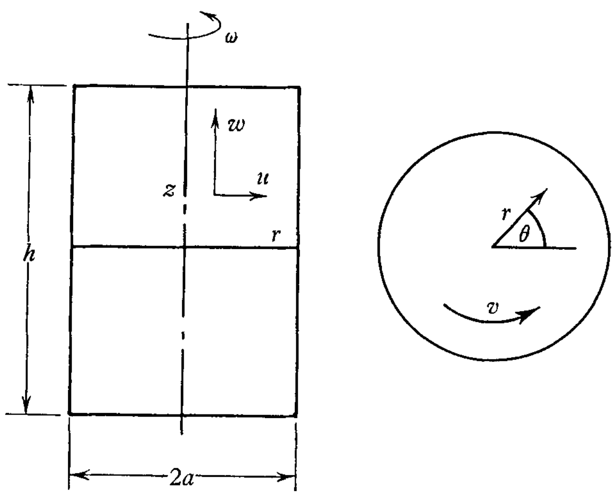

FIGURE 1. Axial section and cross-section of spinning cylinder.

figure 1. The velocity components are v, u, w, respectively. The Navier–Stokes equations in these co-ordinates for a flow having rotational symmetry are

$$\frac{\partial v}{\partial t}+u\left(\frac{\partial v}{\partial r}+\frac{v}{r}\right)+w\frac{\partial v}{\partial z}=\nu\left[\frac{\partial^2 v}{\partial r^2}+\frac{\partial}{\partial r}\left(\frac{v}{r}\right)+\frac{\partial^2 v}{\partial z^2}\right], \tag{1a}$$

$$\frac{\partial u}{\partial t}+u\frac{\partial u}{\partial r}+w\frac{\partial u}{\partial z}-\frac{v^2}{r}+\frac{1}{\rho}\frac{\partial p}{\partial r}=\nu\left[\frac{\partial^2 u}{\partial r^2}+\frac{\partial}{\partial r}\left(\frac{u}{r}\right)+\frac{\partial^2 u}{\partial z^2}\right], \tag{1b}$$

$$\frac{\partial w}{\partial t}+u\frac{\partial w}{\partial r}+w\frac{\partial w}{\partial z}+\frac{1}{\rho}\frac{\partial p}{\partial z}=\nu\left[\frac{\partial^2 w}{\partial r^2}+\frac{1}{r}\frac{\partial w}{\partial r}+\frac{\partial^2 w}{\partial z^2}\right], \tag{1c}$$

$$\frac{\partial(ru)}{\partial r}+\frac{\partial(rw)}{\partial z}=0. \tag{1d}$$

The boundary conditions are $u=w=0$, $v=\omega r$ at $z=\pm\frac{1}{2}h$, and $u=w=0$, $v=a\omega$ at $r=a$, with $u, v=0$ at $r=0$.

Let us assume that at time $t = 0$ the cylinder is started spinning about its axis of rotation with the constant or time-dependent angular velocity ω.

If the cylinder is infinitely long, i.e. $h \to \infty$, the equations (1*b*), (1*c*) and (1*d*) with the corresponding boundary conditions can be satisfied by

$$u = w = 0, \quad \frac{\partial p}{\partial z} = 0, \quad \frac{1}{\rho}\frac{\partial p}{\partial r} = \frac{v^2}{r},$$

and equation (1*a*) reduces to a linear differential equation,

$$\frac{\partial v}{\partial t} = \nu\left(\frac{\partial^2 v}{\partial r^2} + \frac{\partial v/r}{\partial r}\right), \tag{2}$$

where v depends on r and t only. No such solution with $u = w = 0$ is possible if the cylinder has a finite length. In the vicinity of the end walls, $z = \pm\frac{1}{2}h$, the circumferential component v must depend on z and, according to equations (1*b*) and (1*c*), the velocity components u, w must be different from zero. In fact, the fluid particles at the cylinder ends rotate with the velocity of the walls and are therefore subject to centrifugal forces. Because of these centrifugal forces, the particles close to the end walls are driven outwards, creating a secondary flow with velocity components u, w. We can assume, however, with the reservation of a final proof, that the secondary motion u, w is very slow except in a thin boundary-layer region at each of the end walls. Thus, we can divide the entire flow region in two parts, the boundary-layer region close to the end walls and the rest of the flow, which we will call the core flow. A similar flow structure was found by Ludwieg (1951) for the steady flow in a rotating duct, and the following considerations will be analogous to those given by Ludwieg (1951).

2.2. *Approximate equation for the core flow*

Let us use the notation v_0, u_0, w_0, p_0 for the velocity components and the pressure in the core flow. If we apply equation (1*b*) to the core flow, we can neglect the terms containing u, w, according to our assumption that the secondary motion is very slow in the core flow, and we have approximately

$$\frac{1}{\rho}\frac{\partial p_0}{\partial r} = \frac{v_0^2}{r}. \tag{3}$$

From equation (1*c*) we observe that the axial pressure gradient $\partial p_0/\partial z$ is very small; or, within our approximation, we can assume that the pressure is independent of z. But then, according to equation (3), v_0 must be independent of z, and equation (1*a*) applied to the core flow gives

$$\frac{\partial v_0}{\partial t} + u_0\left(\frac{\partial v_0}{\partial r} + \frac{v_0}{r}\right) = \nu\left(\frac{\partial^2 v_0}{\partial r^2} + \frac{\partial v_0/r}{\partial r}\right). \tag{4}$$

Since v_0 is independent of z, it can be seen from (4) that u_0 must also be independent of z. Thus (4) reduces to a partial differential equation in the independent variables r and t.

Before we can solve (4) for the circumferential component v_0, we must have an additional relation which allows us to express the other dependent variable

u_0 in terms of v_0. The required additional relation between u_0 and v_0 will be given by the coupling between boundary-layer flow and core flow.

2.3. *Boundary-layer flow*

Since the flow within the spinning cylinder must be symmetric with respect to the middle plane $z = 0$, we can restrict our analysis to the boundary layer at one of the end walls, say $z = -\frac{1}{2}h$.

The boundary-layer equations can be obtained from the Navier–Stokes equations ($1a$) to ($1d$), applying the usual boundary-layer simplifications. The radial pressure gradient within the boundary layer can be replaced by the pressure gradient of the 'outer' flow, i.e. the core flow in our case. Thus, according to (3),

$$\frac{1}{\rho}\frac{\partial p}{\partial r} = \frac{v_0^2}{r}.$$

The friction forces reduce to $\nu(\partial^2 v/\partial z^2)$, etc. Although the boundary-layer flow is unsteady, we can treat it as a quasi-steady flow, i.e. the local acceleration terms $\partial v/\partial t$, etc., can be neglected. Apart from a very short acceleration period, after the cylinder starts to spin, the local acceleration terms are very small compared to the convective terms. During the acceleration period, the flow at each of the end walls is essentially the same as the flow on an impulsively started rotating disk. The unsteady boundary-layer flow on an impulsively started rotating disk was investigated by Thiriot (1940). According to Thiriot's solution, the duration of the acceleration period is $\approx 2/\omega$, i.e. after a fraction π^{-1} of a revolution the boundary-layer flow is almost steady. We can, therefore, ignore the acceleration period and consider the boundary-layer flow as quasi-steady for all time. The boundary-layer equations are then

$$u\frac{\partial u}{\partial r} + w\frac{\partial u}{\partial z} - \frac{v^2}{r} + \frac{v_0^2}{r} = \nu\frac{\partial^2 u}{\partial z^2}, \tag{5a}$$

$$u\frac{\partial v}{\partial r} + u\frac{v}{r} + w\frac{\partial v}{\partial z} = \nu\frac{\partial^2 v}{\partial z^2}, \tag{5b}$$

$$\frac{\partial(ru)}{\partial r} + \frac{\partial(rw)}{\partial z} = 0. \tag{5c}$$

For convenience we change our co-ordinate system, so that the lower end wall of the cylinder is given by $z = 0$. The boundary conditions, then, are

$$\left.\begin{aligned} v = r\omega, \quad u = 0, \quad w = 0 \quad \text{at} \quad z = 0;\\ v = v_0(r,t), \quad u = 0 \quad \text{at} \quad z = \infty. \end{aligned}\right\} \tag{5d}$$

v_0 enters into our boundary-layer problem twice; first, it occurs in equation ($5a$), and secondly, it enters into one of the boundary conditions. For any given outer flow $v_0(r)$, the boundary-layer flow is determined by the equations ($5a, b, c$) and the boundary conditions ($5d$). Thus, we have a coupling between the boundary-layer flow and the core flow.

The boundary-layer equations ($5a$, b, c) have been the subject of many investigations. von Kármán (1921) considered the flow on a rotating disk in a fluid at rest ($v_0 = 0$) and obtained approximate solutions using the integral method he invented. A more accurate solution to the same problem was calculated by Cochran (1934). The problem of rigid-body fluid rotation over a stationary disk was solved by Bödewadt (1940).

Batchelor (1951), Stewartson (1958), Rogers & Lance (1960) and others investigated the more general problem of a fluid in rigid-body rotation over a rotating disk. A common feature of the above-mentioned flows is that they have similarity solutions, where the velocity components take the form $v = rG(z)$, $u = rF(z)$, $w = H(z)$. These similarity solutions are also solutions of the exact Navier–Stokes equations, since the terms, which are commonly neglected in boundary-layer theory, vanish identically. Ludwieg (1951) and Squire (1953) linearized the boundary-layer equations ($5a, b, c$) for the case of small disturbances about a state of rigid rotation. In the linearized form, the equations ($5a, b, c$) reduce to a set of ordinary differential equations, which are linear.

For general v_0-distributions, when neither linearization nor the assumption of similarity flow is applicable, approximate solutions may be obtained by using the momentum-integral methods. Mack (1962, 1963) has applied the momentum-integral method (1962) and a simplified momentum-integral method (1963) to rotating flows on a stationary disk. The latter method, which makes computations easy, could be extended to our case of rotating flows on a rotating disk. While the momentum-integral method does not give the exact shape of the velocity profiles, it provides fairly good approximations to certain integral values, e.g. the radial mass-flow within the boundary layer, which is

$$M(r) = 2\pi r \rho \int_0^\delta u(r,z)\,dz,$$

where δ is the boundary-layer thickness. When the radial mass-flow distribution $M(r)$ has been determined—for a given distribution of $v_0(r)$—the radial velocity in the core flow, $u_0(r)$, can be found.

Making use of the condition that the total radial mass-flow (within the two boundary layers and the core flow) must be zero, one obtains

$$2\pi r \rho \left[2\int_0^\delta u(r,z)\,dz + hu_0(r)\right] = 0, \tag{6}$$

or

$$-\tfrac{1}{2}hu_0(r) = \int_0^\delta u(r,z)\,dz.$$

Thus, we have a functional dependence

$$u_0(r) = F[v_0(r)]. \tag{7}$$

This means that for any given distribution of $v_0(r)$ we can find the distribution of $u_0(r)$. In principle we could now express u_0 in equation (4) in terms of v_0 making use of the functional dependence (7). But aside from the fact that we cannot give an explicit formula for $u_0(r)$, the relation (7) will be much too complex to enable us to solve (4). Thus we have to confine ourselves to a simple approximation for the relation (7).

2.4. *Approximate formula for* $u_0(r)$

At the beginning of the fluid motion the circumferential component of the core flow, v_0, is zero and the boundary-layer problem reduces to the problem of the rotating disk flow, which was solved by Cochran (1934). According to Cochran's solution we have

$$\int_0^\infty u\,dz = 0{\cdot}443\left(\frac{\nu}{\omega}\right)^{\frac{1}{2}} r\omega, \tag{8}$$

and hence, from equation (6),

$$-\tfrac{1}{2}hu_0 = 0{\cdot}443\,(\nu/\omega)^{\frac{1}{2}}\,r\omega. \tag{9}$$

If on the other hand the fluid finally attains the state of rigid rotation ($v_0 = r\omega$) the boundary-layer equations (5) have the trivial solution $v = r\omega$, $u = w = 0$ and hence $u_0 = 0$.

The simplest possible approximation for general v_0 distributions then is to assume that

$$-\tfrac{1}{2}hu_0 = 0{\cdot}443\,(\nu/\omega)^{\frac{1}{2}}\,(r\omega - v_0), \tag{10}$$

which is a linear interpolation between the two extreme cases. We can test the validity of this approximation in a few other cases. If the core flow is almost a rigid-body rotation with the angular velocity ω, i.e. $v_0 = r\omega + v_0'$ and $v_0' \ll r\omega$, the boundary-layer equations ($5a, b, c$) can be linearized. In doing this we transform

$$v_0 = r\omega + v_0', \quad u = u', \quad v = r\omega + v', \quad w = w', \tag{11}$$

where the primed quantities are small compared with $r\omega$. Substituting (11) into ($5a, b$) and neglecting terms of higher than first order in the primed quantities, equations ($5a$, b) become

$$\nu(\partial^2 v'/\partial z^2) - 2\omega u' = 0, \quad \nu(\partial^2 u'/\partial z^2) + 2\omega(v' - v_0') = 0. \tag{12}$$

These linearized equations were used by Ludwieg (1951) for the boundary-layer flow in a rotating duct. With the boundary conditions

$$v' = 0, \quad u' = 0, \quad \text{at} \quad z = 0; \quad v' = v_0', \quad u' = 0, \quad \text{at} \quad z = \infty,$$

equations (12) are satisfied by

$$v' = v_0'[1 - \cos\{(\omega/\nu)^{\frac{1}{2}} z\}\exp\{-(\omega/\nu)^{\frac{1}{2}} z\}], \quad u' = -v_0' \sin\{(\omega/\nu)^{\frac{1}{2}} z\}\exp\{-(\omega/\nu)^{\frac{1}{2}} z\}. \tag{13}$$

For the radial component in the core flow u_0 we have, according to (6),

$$-\tfrac{1}{2}hu_0(r) = \int_0^\infty u'\,dz = -\tfrac{1}{2}v_0'\,(\nu/\omega)^{\frac{1}{2}}.$$

If we replace v_0' according to (11) by $-(r\omega - v_0)$, we have

$$-\tfrac{1}{2}hu_0 = 0{\cdot}500(\nu/\omega)^{\frac{1}{2}}\,(r\omega - v_0). \tag{14}$$

This formula for u_0 is similar to the linear interpolation formula (10) except that the factor of 0·500 in (14) is 13 % larger than the factor 0·443 in (10), so that the error in the approximate formula (10) in this case is 13 %. For the case when the outer flow is a rigid rotation with the angular velocity Ω, i.e. $v_0 = r\Omega$, the boundary-layer equations (5) have been solved by Rogers & Lance (1960) for several values of Ω/ω. According to the solution of Rogers & Lance, the radial flow integral is given by

$$-\tfrac{1}{2}hu_0 = \int_0^\infty u\,dz = (\nu/\omega)^{\frac{1}{2}} r\omega f(\Omega/\omega), \tag{15}$$

where the function $f(\Omega/\omega)$ is shown in figure 2. If we apply our approximation formula (10) to the case when $v_0 = r\Omega$, we get

$$-\tfrac{1}{2}hu_0 = 0{\cdot}443(\nu/\omega)^{\frac{1}{2}} r\omega(1-\Omega/\omega). \tag{16}$$

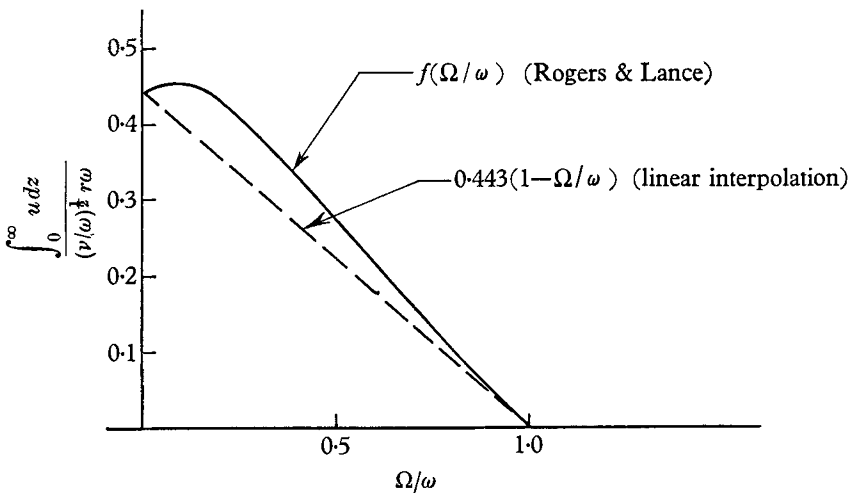

FIGURE 2. Radial flow integral as a function of Ω/ω. ———, Rogers & Lance (exact); — — —, linear interpolation, [$0{\cdot}443(1-\Omega/\omega)$].

Thus the function $f(\Omega/\omega)$ has to be compared with the approximate expression $0{\cdot}443\ (1-\Omega/\omega)$, which is shown by the dotted line in figure 2. The agreement is good enough for us to consider equation (10) a reasonable approximation in this case also. Whether or not equation (10) is approximately valid for the actual velocity profiles $v_0(r,t)$ can be checked after obtaining the solution for $v_0(r,t)$. A calculation of the radial flow integral for some of the obtained velocity profiles $v_0(r,t)$ has been done, based on the simplified momentum-integral method of Mack (1963). The u_0 values obtained from these calculations have been compared with the approximate values from equation (10) and the agreement found to be good within the accuracy of the momentum-integral method, which is about 15 %. Thus, we can conclude that the error of the approximation (10) for u_0 is probably not larger than 15 %.

Using the notation $Re = a^2\omega/\nu$ for the Reynolds number, equation (10) can be written as

$$u_0 = -0{\cdot}443(2a/h)\,Re^{-\frac{1}{2}}(r\omega - v_0) \tag{17}$$

or, with the notation

$$k = 0{\cdot}443\,(2a/h)Re^{-\frac{1}{2}}, \tag{18}$$

as

$$u_0 = -k(r\omega - v_0). \tag{19}$$

2.5. *Solution for* $v_0(r,t)$

After substituting (19) into (4) the equation for v_0 is

$$\frac{\partial v_0}{\partial t}+k(v_0-r\omega)\left(\frac{\partial v_0}{\partial r}+\frac{v_0}{r}\right)=\nu\left(\frac{\partial^2 v_0}{\partial r^2}+\frac{\partial v_0/r}{\partial r}\right), \tag{20}$$

where $k = 0{\cdot}443\,(2a/h)\,Re^{-\frac{1}{2}}$. The initial and boundary conditions are

$$v_0 = 0 \quad \text{for} \quad t<0, \quad v_0 = a\omega \quad \text{for} \quad r=a \quad \text{and} \quad t \geqslant 0.$$

Let us restrict our analysis at this point to the case of constant ω (i.e. the cylinder is started spinning with constant angular velocity ω at $t = 0$). In many cases, we can neglect the friction terms on the right-hand side of equation (20) as compared with the convection terms. To see this we multiply equation (20) by $1/a\omega^2$ and, introducing the dimensionless variables $v^* = v_0/a\omega$, $r^* = r/a$ equation (20) becomes

$$\frac{\partial v^*}{\partial \omega t}+k(v^*-r^*)\left(\frac{\partial v^*}{\partial r^*}+\frac{v^*}{r^*}\right)=\frac{1}{Re}\left(\frac{\partial^2 v^*}{\partial r^{*2}}+\frac{\partial}{\partial r^*}\frac{v^*}{r^*}\right), \tag{21}$$

with the boundary conditions

$$v^* = 1 \quad \text{for} \quad r^* = 1 \quad \text{and} \quad \omega t \geqslant 0.$$

It can be seen from equation (21) that the solution v^* is a function of $k\omega t$, r^* and the dimensionless parameter $kRe = 0{\cdot}443\,(2a/h)\,Re^{\frac{1}{2}}$, i.e.

$$v^* = f(r^*, k\omega t, kRe).$$

If $kRe = 0{\cdot}443\ 2aRe^{\frac{1}{2}}/h \gg 1$, then the viscous terms at the right-hand side of (21) become small except for small times when the gradient $\partial v^*/\partial r^*$ is large near the wall $r^* = 1$. For not too small times and $kRe \gg 1$ we can therefore neglect the viscous terms and the solution of the inviscid equation is

$$\left.\begin{aligned} v^* &= (r^* e^{2k\omega t}-1/r^*)/(e^{2k\omega t}-1) \quad &\text{for} \quad r^* \geqslant e^{-k\omega t},\\ v^* &= 0 \quad &\text{for} \quad r^* \leqslant e^{-k\omega t}.\end{aligned}\right\} \tag{22}$$

A plot of the v^*-profiles (equation (22)) for different times is shown in figure 3.

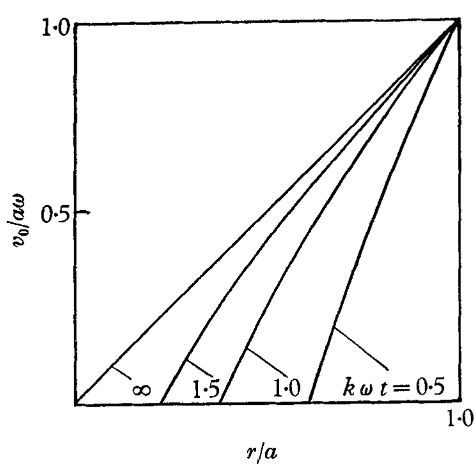

FIGURE 3. Velocity profiles for the core flow.

It is remarkable that the solution (22) also satisfies the complete equation (21) with viscous terms except at the point $r^* = e^{-k\omega t}$ where the first derivative is discontinuous. The inviscid equation is of the first order in the derivatives and hence only the solution function has to be continuous, while the complete equation has second-order derivatives and the solution must have continuous derivatives. The effect of the viscosity, therefore, will be to smooth the corner at $r^* = e^{-k\omega t}$. With the solution (22) for v_0 the other flow components u_0, w_0 can be obtained at once. First of all we have, from (19)

$$u_0 = -k(r\omega - v_0).$$

From the equation of continuity ($1d$) and the condition that the flow must be symmetric about the plane $z = 0$, it follows that

$$w_0 = -\frac{z}{r}\frac{\partial(ru_0)}{\partial r}. \tag{23}$$

Within the core flow we can distinguish two regions.

$$\text{Region 1: } 0 < r/a < e^{-k\omega t};$$

$$\text{Region 2: } e^{-k\omega t} < r/a < 1.$$

According to equation (22) the particles in region 1 do not rotate (i.e. $v_0 = 0$) while the particles in region 2 rotate with the velocity $v_0 = a\omega v^*$ given by equation (22). Regions 1 and 2 are separated by the cylindrical front $r/a = e^{-k\omega t}$, which moves towards the axis $r = 0$.

It can be shown that the particles in region 1, i.e. the particles ahead of the moving front, remain ahead of it until they hit one of the boundary layers at the end walls $z = \pm\frac{1}{2}h$. To see this, we compute the trajectories of the particles in region 1. From $v_0 = 0$ it follows that $u_0 = -kr\omega$ and $w_0 = 2kz\omega$ (equation (23)). From

$$dr/dt = u_0 = -kr\omega, \quad dz/dt = w_0 = 2kz\omega, \tag{24}$$

we obtain by integration

$$r = r_0 e^{-k\omega t}, \quad z = z_0 e^{2k\omega t} = z_0(r_0/r)^2, \tag{25}$$

where (r_0, z_0) is the particle position at $t = 0$. The trajectories (25) are entirely in region 1, so that the solution (25) is compatible with the supposition $v_0 = 0$.

Thus we obtain the following flow picture: after the cylinder is started at $t = 0$, the fluid particles move along hyperbolas given by (25) until they hit the boundary layer at one of the end walls $z = \pm\frac{1}{2}h$; in the boundary layer the flow direction changes rapidly, the particles acquire rotational motion and are thrown radially outwards until they emerge from the boundary layer at some distance behind the moving front $r/a = e^{-k\omega t}$, now having a rotational component v_0 according to equation (22). The rest of the trajectories are entirely in region 2.

Actually, this flow picture will be modified slightly. The particles can acquire rotational motion in region 1 by the action of the viscous force term in equation (21) which has been neglected so far. This will also slightly modify the trajectories given by equation (25).

2.6. *Equations for the angular momentum*

Of particular interest is the total angular momentum of the liquid within the cylinder, which is

$$I = \rho h . 2\pi \int_0^a r^2 v_0 dr. \tag{26}$$

An equation for the angular momentum I can be obtained from equation (20). To this end, we multiply equation (20) by r^2 and integrate from $r = 0$ to $r = a$. If we consider that

$$\frac{\partial v_0}{\partial r} + \frac{v_0}{r} = \frac{1}{r}\frac{\partial (rv_0)}{\partial r},$$

this gives

$$\left[\frac{\partial}{\partial t}\int_0^a r^2 v_0 dr + k\int_0^a (rv_0 - r^2\omega)\frac{\partial (rv_0)}{\partial r} dr\right] = \nu \int_0^a r^2 \frac{\partial}{\partial r}\left(\frac{1}{r}\frac{\partial (rv_0)}{\partial r}\right) dr. \tag{27}$$

The second integral consists of two terms: the first one gives

$$k\int_0^a rv_0 \frac{\partial (rv_0)}{\partial r} dr = [\tfrac{1}{2}k\,(rv_0)^2]_0^a,$$

while the second term can be integrated by parts to give

$$-k\omega \int_0^a r^2 \frac{\partial (rv_0)}{\partial r} dr = [-k\omega r^3 v_0]_0^a + 2k\omega \int_0^a r^2 v_0 dr.$$

Considering that $v_0 = a\omega$ for $r = a$, the second integral of equation (27) gives

$$k\int (rv_0 - r^2\omega)\frac{\partial (rv_0)}{\partial r} dr = -\tfrac{1}{2}ka^4\omega^2 + 2k\omega\int_0^a r^2 v_0 dr.$$

The integral at the right side of equation (27) becomes, after integration by parts,

$$\nu \int_0^a r^2 \frac{\partial}{\partial r}\left(\frac{1}{r}\frac{\partial (rv_0)}{\partial r}\right) dr = \nu\left[r\frac{\partial (rv_0)}{\partial r}\right]_0^a - \nu[2rv_0]_0^a = \nu a^3\left(\frac{\partial (v_0/r)}{\partial r}\right)_{r=a}.$$

We thus get the equation

$$\frac{d}{dt}\int_0^a r^2 v_0 dr - \tfrac{1}{2}k\,a^4\omega^2 + 2k\omega\int_0^a r^2 v_0 dr = \nu a^3\left(\frac{\partial (v_0/r)}{\partial r}\right)_{r=a}. \tag{28}$$

According to (26) the value of the angular momentum is

$$I = 2\pi h\rho \int_0^a r^2 v_0 dr.$$

In the final state, i.e. when the liquid approaches rigid-body rotation $v_0 = r\omega$, the angular momentum becomes

$$I_\infty = 2\pi h\rho \int_0^a r^3 \omega dr = 2\pi h\rho\,(a^4\omega/4). \tag{29}$$

The ratio of the angular momentum I to its final value I_∞ is then

$$\frac{I}{I_\infty} = \int_0^a r^2 v_0\, dr \Big/ \tfrac{1}{4}a^4\omega.$$

After dividing equation (28) by $\frac{1}{4}a^4\omega$, it can be written

$$\frac{d}{dt}\left(\frac{I}{I_\infty}\right)+2k\omega\left[\frac{I}{I_\infty}-1\right]=\frac{4\nu}{a\omega}\left(\frac{\partial(v_0/r)}{\partial r}\right)_{r=a}. \tag{30}$$

If we again neglect the viscous term at the right side of equation (30), the equation can be integrated at once to give

$$I/I_\infty=(1-e^{-2k\omega t}). \tag{31}$$

This result, of course, could also have been obtained by integration from the solution (22) for the velocity profiles $v^*=v_0/a\omega$.

In order to improve the solution (31) we have to take into account the friction term

$$\frac{4\nu}{a\omega}\left(\frac{\partial(v_0/r)}{\partial r}\right)_{r=a}$$

of equation (30). This can be done within a fairly good approximation by assuming the approximate shape of the velocity profiles $v_0(r)$ and expressing

$$[\partial(v_0/r)/\partial r]_{r=a} \quad \text{in terms of} \quad I/I_\infty.$$

Since the contribution of the viscous term is small, it appears reasonable to assume that the v_0-profiles will have essentially the same shape as the profiles that we have obtained as solutions of the inviscid equation. Thus, we may assume profiles of the form

$$\left.\begin{aligned}&v_0/a\omega=(A^2r/a-a/r)/(A^2-1)\quad\text{for}\quad r/a>A^{-1},\\&v_0/a\omega=0\quad\text{for}\quad r/a<A^{-1},\end{aligned}\right\} \tag{32}$$

where A is a function of time. For the case where the viscous term is wholly neglected, the solution for $v_0/a\omega$ was given, according to equation (22), by the profiles (32) with $A=e^{k\omega t}$.

It might be mentioned that the v_0 profiles (32) satisfy the compatability condition

$$\left(\frac{\partial^2v_0}{\partial r^2}+\frac{\partial(v_0/r)}{\partial r}\right)_{r=a}=0, \tag{33}$$

which is obtained by evaluating equation (20) at $r=a$. Using the v_0 profiles given by (32) we have

$$\left(\frac{\partial(v_0/r)}{\partial r}\right)_{r=a}=\frac{2\omega}{a}\bigg/(A^2-1), \tag{34}$$

while

$$I/I_\infty=1-A^{-2}. \tag{35}$$

Thus, from (34) and (35) we obtain

$$\left(\frac{\partial(v_0/r)}{\partial r}\right)_{r=a}=\frac{2\omega}{a}\left[\frac{I_\infty}{I}-1\right]. \tag{36}$$

Inserting (36) into (30) we have

$$\frac{d}{dt}\left(\frac{I}{I_\infty}\right)+2k\omega\left[\frac{I}{I_\infty}-1\right]=\frac{8\nu}{a^2}\left[\frac{I_\infty}{I}-1\right],$$

or, after dividing by ω,

$$\frac{d(I/I_\infty)}{d\omega t}+2k\left[\frac{I}{I_\infty}-1\right]=\frac{8}{Re}\left[\frac{I_\infty}{I}-1\right]. \tag{37}$$

It should be mentioned that the approximation for $[\partial(v_0/r)/\partial r]_{r=a}$ given by equation (36) is not very sensitive to the special choice of velocity profiles. Although the very early v_0-profiles are somewhat different from those given in equation (32), the expression (36) is still a good approximation.

It can be shown from equation (37) that for sufficiently small times the friction term is dominant however large kRe is. The equation for v_0 is then

$$\partial v_0/\partial t = \nu(\partial^2 v_0/\partial r^2), \tag{38}$$

which is obtained from equation (20) by neglecting the convection terms and $\nu\partial(v_0/r)/\partial r$ compared with $\nu(\partial^2 v_0/\partial r^2)$. The solution of (38) is

$$v_0(r,t) = a\omega\left[1-\frac{2}{\sqrt{\pi}}\int_0^{(a-r)/\sqrt{(\nu t)}} e^{-y^2}dy\right]. \tag{39}$$

With the velocity profiles given by equation (39) one would have

$$\left(\frac{\partial(v_0/r)}{\partial r}\right)_{r=a} = \frac{8}{\pi}\frac{\omega}{a}\frac{I_\infty}{I} = 2{\cdot}54\frac{\omega}{a}\frac{I_\infty}{I},$$

while equation (36) gives approximately

$$\left(\frac{\partial(v_0/r)}{\partial r}\right)_{r=a} = 2\frac{\omega}{a}\frac{I_\infty}{I},$$

since for small times $I_\infty/I \gg 1$. Thus, we see that equation (36) is a reasonably good approximation even for the very early velocity profiles.

The differential equation (37) now has to be solved for the initial condition $I/I_\infty = 0$ at $t = 0$. The solution for I/I_∞ can be given implicitly

$$2k\omega t = \frac{-1}{1+4/kRe}\left[\log(1-I/I_\infty)+\frac{4}{kRe}\log(1+\tfrac{1}{4}kRe\,I/I_\infty)\right]. \tag{40}$$

For $kRe \to \infty$ the solution (40) reduces to $1-I/I_\infty = e^{-2k\omega t}$, i.e. the inviscid solution given by (31). For very small times, or more precisely for $I/I_\infty \ll 1$ and $\frac{1}{4}kReI/I_\infty \ll 1$, equation (40) gives $I/I_\infty \approx 4(\omega t/Re)^{\frac{1}{2}}$, i.e. the angular momentum increases as the square root of t.

The validity of the preceding results is restricted to the case where the angular velocity of the cylinder, ω, remains constant after the cylinder is started. If ω is not constant, it is advantageous to introduce the dimensionless quantity

$$I^* = \frac{I}{I_0} = \frac{4}{a^4\omega_0}\int_0^a v_0 r^2\,dr, \tag{41}$$

where ω_0 is a constant reference angular velocity and I_0 is a reference angular momentum,

$$I_0 = 2\pi\rho h\int_0^a \omega_0 r^3\,dr,$$

the latter corresponding to a rigid rotation with angular velocity ω_0. Dividing equation (28) by $\frac{1}{4}a^4\omega_0^2$ and substituting $\{\partial(v_0/r)/\partial r\}_{r=a}$ according to equation (36) we have

$$\frac{dI^*}{d\omega_0 t}+2k_0\left(\frac{\omega}{\omega_0}\right)^{\frac{1}{2}}\left[I^*-\frac{\omega}{\omega_0}\right] = \frac{8}{Re_0}\frac{\omega}{\omega_0}\left[\frac{1}{I^*}\frac{\omega}{\omega_0}-1\right], \tag{42}$$

where $\quad Re_0 = a^2\omega_0/\nu \quad$ and $\quad k_0 = 0{\cdot}443\,(2a/h)\,(Re_0)^{-\frac{1}{2}}.$

Equation (42) has been used to calculate the spin decay of a liquid-filled shell. If a shell containing a liquid-filled cylindrical cavity is started impulsively to spin about its axis of rotation, the liquid continuously absorbs angular momentum, thus reducing the spin until the liquid finally attains rigid-body rotation. Let A be the axial moment of inertia of the empty shell, ω the instantaneous angular velocity and I the angular momentum of the liquid; then, from conservation of angular momentum,

$$I + \omega A = \text{const.} = \omega_0 A, \tag{43}$$

where ω_0 is the initial angular velocity when the liquid is at rest. According to (43) we can express I by ω

$$I = A\omega_0(1-\omega/\omega_0),$$

or using the definition (41),

$$I^* = (A\omega_0/I_0)(1-\omega/\omega_0). \tag{44}$$

After inserting (44) into (42) we get a differential equation for I^* (or ω/ω_0) which may be solved by numerical integration.

2.7. *Turbulent boundary-layer flow*

In §§2.3 and 2.4 we have assumed that the boundary-layer flow at the cylinder ends is laminar. This assumption is valid for Reynolds numbers $Re = a^2\omega/\nu$ up to about 3×10^5 (see e.g. Schlichting 1958). For Reynolds numbers greater than 3×10^5 the boundary-layer flow will be turbulent and the radial mass flow and hence u_0 will be different from the laminar case. According to the solution of von Kármán (1921) for the turbulent boundary-layer flow on a rotating disk, the radial flow integral is

$$\int_0^\infty u\,dz = 0{\cdot}035\, r^{\frac{3}{5}}\,(\nu/\omega)^{\frac{1}{5}}\, r\omega. \tag{45}$$

This formula is analogous to equation (8), which corresponds to the laminar case.

Using again the notation $Re = a^2\omega/\nu$ for the Reynolds number, equation (45) can be written as

$$\int_0^\infty u\,dz = 0{\cdot}035a(Re)^{-\frac{1}{5}}\,(r\omega)^{\frac{8}{5}}/(a\omega)^{\frac{3}{5}}. \tag{46}$$

By arguments similar to those used in §2.4 for the laminar boundary layer, it seems appropriate to generalize equation (46) to

$$\int_0^\infty u\,dz = 0{\cdot}035a(R-e)^{-\frac{1}{5}}\,(r\omega - v_0)^{\frac{8}{5}}/(a\omega)^{\frac{3}{5}}. \tag{47}$$

According to equation (6) we then have for the radial component of the core flow:

$$u_0(r) = -0{\cdot}035(2a/h)\,(Re)^{-\frac{1}{5}}\,(r\omega - v_0)^{\frac{8}{5}}/(a\omega)^{\frac{3}{5}}. \tag{48}$$

Equation (48) is analogous to equation (17). With u_0 obtained from equation (48) equation (4) for the core flow becomes

$$\frac{\partial v_0}{\partial t} - \frac{k_t}{(a\omega)^{\frac{3}{5}}}\,(r\omega - v_0)^{\frac{8}{5}}\left(\frac{\partial v_0}{\partial r} + \frac{v_0}{r}\right) = \nu\left[\frac{\partial^2 v_0}{\partial r^2} + \frac{\partial(v_0/r)}{\partial r}\right], \tag{49}$$

where

$$k_t = 0{\cdot}035(2a/h)\,(Re)^{-\frac{1}{5}}. \tag{50}$$

Analogous to the procedure described in §2.6, we find the equation for the angular momentum by multiplying equation (49) by $4r^2/a^4\omega_0^2$ and integrating over r. If we further introduce the dimensionless quantity I^* according to equation (41) we finally have

$$\frac{dI^*}{d\omega_0 t} - \frac{k_t}{(a\omega)^{\frac{2}{5}}} \frac{4}{a^4\omega_0^2} \int_0^a r(r\omega - v_0)^{\frac{8}{5}} \left(\frac{\partial(rv_0)}{\partial r}\right) dr = \frac{4\nu}{a\omega_0} \left(\frac{\partial(v_0/r)}{\partial r}\right)_{r=a}. \tag{51}$$

The integral in equation (51) cannot be evaluated as it could for the laminar case, without knowing how v_0 depends on r. Only for small times when the v_0 profiles are restricted to a narrow zone near the wall $r = a$, can we approximate r in the integral by a and obtain

$$\int_0^a a(a\omega - v_0)^{\frac{8}{5}} \frac{\partial(av_0)}{\partial r} dr = \left[\frac{-5}{13} a^2(a\omega - v_0)^{\frac{13}{5}}\right]_0^a = \frac{5}{13} a^2(a\omega)^{\frac{13}{5}}.$$

Inserting the last result into (51) and using, for the viscous term on the right side, the same approximation as in equation (42), we obtain

$$\frac{dI^*}{d\omega_0 t} - \frac{20}{13} k_{t0} \left(\frac{\omega}{\omega_0}\right)^{\frac{9}{5}} = \frac{8}{(Re)_0} \left(\frac{\omega}{\omega_0}\right) \left[\frac{1}{I^*} \frac{\omega}{\omega_0} - 1\right], \tag{52}$$

where again $(Re)_0 = a^2\omega_0/\nu$ and $k_{t0} = 0{\cdot}035\,(2a/h)\,(Re_0)^{-\frac{1}{5}}$. In order to evaluate the integral in equation (51) for later times, when the assumption $r \approx a$ is no longer valid, we have to make assumptions about the shape of the velocity profiles $v_0(r)$. We may assume that the velocity profiles are again given roughly by equation (32). These profiles, at least, satisfy the compatibility condition (33), i.e. they are correct near the wall.

Using the v_0 profiles given by (32) the integral in equation (51) can be evaluated and expressed by I^*. After some lengthy calculation, one finally obtains from equation (51)

$$\frac{dI^*}{d\omega_0 t} - k_{t0} \left(\frac{\omega}{\omega_0}\right)^{\frac{9}{5}} \cdot \frac{(1 - I^*\omega_0/\omega)^{\frac{8}{5}}}{(I^*\omega_0/\omega)^{\frac{13}{5}}} \cdot 4 \int_0^{I^*\omega_0/\omega} \frac{x^{\frac{8}{5}}}{(1-x)^{\frac{3}{10}}} dx = \frac{8}{Re_0} \frac{\omega}{\omega_0} \left[\frac{1}{I^*} \frac{\omega}{\omega_0} - 1\right]. \tag{53}$$

For small times, i.e. as long as $I^*\omega_0/\omega \ll 1$, the integral approximates to

$$\tfrac{5}{13}(I^*\omega_0/\omega)^{\frac{13}{5}},$$

while $(1 - I^*\omega_0/\omega)^{\frac{8}{5}} \approx 1$, and equation (53) reduces to equation (52). Equation (53) has been used to calculate the spin decay of a liquid-filled shell for $Re_0 > 3 \times 10^5$.

3. Comparison with experiments

In order to test the analysis given in the preceding section, some of the theoretical predictions have been compared with existing experimental data. A detailed description of the experimental arrangements is given by Karpov (1962). A quantity which has been measured directly is the axial spin decay of liquid-filled shells fired from a gun. After the shell leaves the gun, the angular velocity decreases continuously. The decrease of angular velocity is caused by absorption of angular momentum in the liquid and by the torque due to air friction. The contribution of the air friction, which is usually small, can be determined separately by observation of the spin decrease of the empty shell. The difference, which is due to absorption of angular momentum, has been plotted for two typical cases in figures 4 and 5. For comparison, the theoretical curves are plotted in the same diagram and also the curves obtained from the

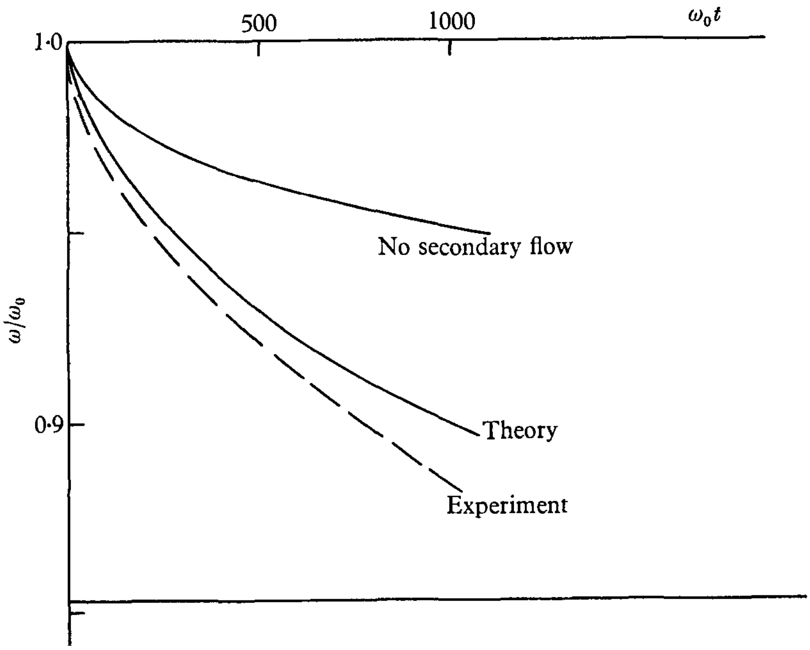

$\omega(\infty)/\omega_0 = 0{\cdot}853$

FIGURE 4. Spin decay for laminar boundary-layer flow. $Re = 1{\cdot}76 \times 10^5$, $h/2a = 2{\cdot}68$.

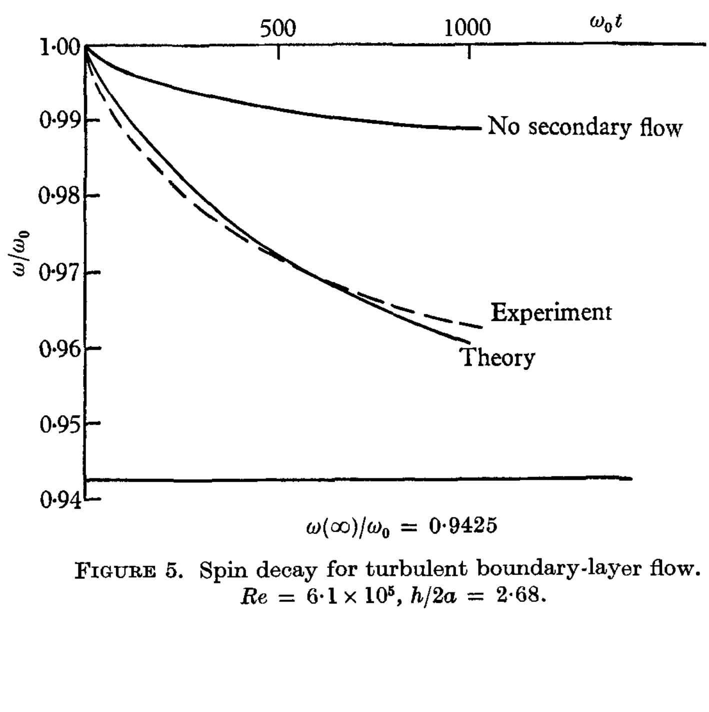

$\omega(\infty)/\omega_0 = 0{\cdot}9425$

FIGURE 5. Spin decay for turbulent boundary-layer flow. $Re = 6{\cdot}1 \times 10^5$, $h/2a = 2{\cdot}68$.

theory without secondary flow. The fineness ratio of the cylindrical cavity was in both cases $h/2a = 2{\cdot}68$. For fineness ratios smaller than 2·68 the effect of the secondary flow would be even more pronounced.

The Reynolds number for the case plotted in figure 4 was $Re = 1{\cdot}76 \times 10^5$ so that a laminar boundary-layer flow could be assumed, while for the case of figure 5 the Reynolds number of $Re = 6{\cdot}1 \times 10^5$ was above critical and therefore the formula for turbulent boundary-layer flow was applied.

In addition to observations of spin decay, experiments have been done to observe the secondary flow itself. To this end an impulsive spin generator was designed which is described by Stoller (1960). The spin generator consisted of a liquid-filled cylinder with transparent walls which could be started impulsively to spin about its axis. A suspension of small particles was dissolved in the liquid, the specific gravity of the particles being the same as that of the liquid. The trajectories of the particles could be observed with the aid of a motion camera. For this type of observation, of course, only transparent liquids could be used.

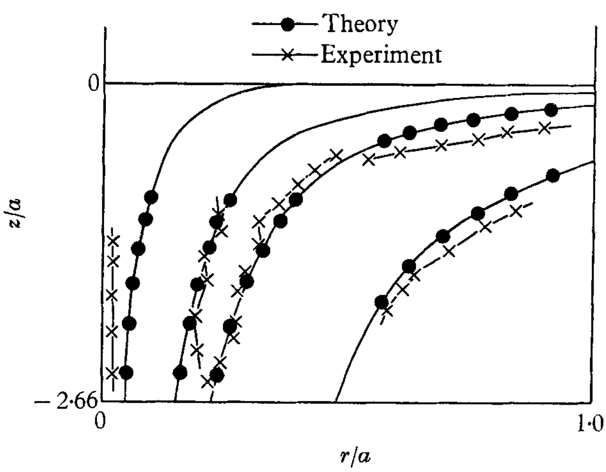

FIGURE 6. Particle trajectories and position of particles at 0·25 sec intervals.

Figure 6 shows some of the observed particle trajectories, or rather the first part of them, and the particle positions at constant time intervals. Close to the observed trajectories, theoretical trajectories and particle positions according to equation (25) are plotted. The agreement is reasonably good. Some deviations can be explained by the fact that the Reynolds number of the experimental flow was rather low ($Re = 1{\cdot}83 \times 10^4$) while the theoretical prediction is based on the assumption of high Reynolds numbers, where the viscous forces in the core flow can be neglected.

The author is grateful to Dr F. D. Bennett and Dr R. Sedney for advice and helpful discussions, and to Dr B. G. Karpov, who made the experimental data accessible.

REFERENCES

Batchelor, G. K. 1951 *Quart. J. Mech. Appl. Math.* **4**, 29.

Bödewadt, U. T. 1940 *Z. angew. Math. Mech.* **20**, 241.

Cochran, W. G. 1934 *Proc. Camb. Phil. Soc.* **30**, 365.

Karpov, B. G. 1962 *Ballistic Research Laboratories Rep.* no. 1171.

Ludwieg, H. 1951 *Ingenieur-Archiv*, **19**, 296.

Mack, L. M. 1962 *Jet Prop. Lab. Tech. Rep.* 32–224.

Mack, L. M. 1963 *Jet Prop. Lab. Tech. Rep.* 32–366.

Rogers, M. H. & Lance, G. N. 1960 *J. Fluid Mech.* **7**, 617.

Schlichting, H. 1958 *Grenzschicht-Theorie,* Karlsruhe: Verlag G. Braun.

Squire, H. B. 1953 *Aero. Res. Counc., Lond.*, 16,021.

Stewartson, K. 1958 *Boundary Layer Research Symposium*, Freiburg, pp. 59–71. Berlin: Springer Verlag.

Stewartson, K. 1959 *J. Fluid Mech.* **5**,

Stoller, H. M. 1960 *Ballistic Research Laboratories Tech. Note* 1355.

Thiriot, K. H. 1940 *Z. angew. Math. Mech.* **20**, 1.

v. Kármán, T. 1921 *Z. angew. Math. Mech.* **1**, 233.